Materials Letters 255 (2019) 126587

Contents lists available at ScienceDirect

Materials Letters

journal homepage: www.elsevier.com/locate/mlblue

Highly anisotropic nanocellular polymers based on tri-phasic blends of PMMA with two nucleating agents

Victoria Bernardo [a,*], Judith Martin-de Leon [a], Miguel Angel Rodriguez-Perez [a,b]

[a] Cellular Materials Laboratory (CellMat), Condensed Matter Physics Department, University of Valladolid, Valladolid, Spain
[b] Instituto BIOECOUVA, Universidad de Valladolid, Valladolid, Spain

ARTICLE INFO

Article history:
Received 17 May 2019
Received in revised form 14 August 2019
Accepted 25 August 2019
Available online 26 August 2019

Keywords:
Nanocellular polymer
Gas dissolution foaming
Nanoparticles
Nanostructuration
PMMA
Anisotropy

ABSTRACT

One strategy to produce nanocellular polymers is the use of nucleating species to promote nucleation. Whereas two-phase systems are widely studied, tri-phasic blends with two nucleating agents are uncommonly investigated. In this work, nanocellular polymers are obtained using tri-phasic blends of polymethylmethacrylate (PMMA) with two nucleating agents: needle-like sepiolites and a polymethylmethacrylate-polybutylacrylate-polymethylmethacrylate (MAM) block copolymer. Blends of PMMA with different concentrations of MAM and a fixed amount of sepiolites are produced by extrusion. Results show that at low MAM contents (1 wt%), the nucleation is a combination of the action of the two additives, but the addition of sepiolites induces the appearance of anisotropic structures. Meanwhile, at high MAM concentrations (10 wt%), MAM nanostructuration controls the nucleation and sepiolites increase the anisotropy. The alignment of the MAM micelles and the sepiolites in the extrusion direction promotes coalescence in this direction, leading to highly anisotropic nanocellular structures. Mean cell sizes of 100–300 nm and an average anisotropy ratio of 2.77 are obtained thanks to the combined effect of MAM and sepiolites.

1. Introduction

Nanocellular polymers are characterized by cell sizes from tens to hundreds of nanometers [1]. They have aroused great attention due to the potential applications of a polymer with nanometric cells [2–4]. Nowadays, much research in this area is focused on finding new systems allowing the production of nanocellular polymers with tunable structures.

One production strategy is the use of nucleating species, such as nanoparticles [5–10] or nanostructured polymer blends [11–16], to increase the nucleation and reduce the cell size. For instance, in the work of Costeux et al. [17] the cell nucleation density of polymethylmethacrylate (PMMA) was enhanced three orders of magnitude using silica nanoparticles, obtaining nanocellular materials with cell sizes of 100 nm and cell densities exceeding 10^{16} cells/cm^3. Regarding the approach of nanostructured polymer blends, the addition of polymethylmethacrylate-polybutylacrylate-polymethylmethacrylate (MAM) block copolymer in a PMMA matrix results in nanometric micelles that act as efficient nucleating agents, as Reglero and coworkers [18] and later Pinto et al. [19] demonstrated. Nucleation densities of 10^{14} nuclei/cm^3 combined with cell sizes of 150–200 nm were obtained with this approach. Although the literature about the effect of one nucleating agent is relatively vast, as far as the authors know, there are still no previous reports on the combined action of more than one nucleating agent.

In this work, we investigate the combined effect of two nucleating agents for the production of nanocellular PMMA. MAM and nanometric sepiolites were used as nucleating species. As aforementioned, MAM is well-known for being a good nucleating agent in the production of nanocellular polymers [20]. Meanwhile, sepiolites have been used successfully for producing nanocellular PMMA [21], and also to induce the formation of anisotropic nanocellular structures [22], which are of great interest due to the enhancement of mechanical properties in the anisotropy direction.

This paper aims at analyzing the resultant cellular structures when the two nucleating agents are combined. Also, highly anisotropic cellular structures are obtained as a result of the two additives. The mechanisms of anisotropy formation are also discussed.

* Corresponding author.
E-mail address: vbernardo@fmc.uva.es (V. Bernardo).

https://doi.org/10.1016/j.matlet.2019.126587
0167-577X/

2. Experimental

2.1. Materials

PMMA V825T (M_n = 43 kg/mol, M_w = 83 kg/mol) was kindly supplied by ALTUGLAS® International. Sepiolites (needle-like magnesium silicate nanoparticles) modified with a quaternary ammonium salt [23] were kindly provided by Tolsa S.A (Spain). MAM block copolymer Nanostrength M52 (M_n = 44 kg/mol, M_w = 75 kg/mol, 52 wt% of PBA [20]) was kindly supplied by Arkema. Medical grade carbon dioxide (CO_2) (99.9% purity) was used as the blowing agent.

2.2. Solid blends production

Two series of blends were produced: binary PMMA/MAM blends with two ratios of MAM (1 and 10 wt%) and tri-phasic blends of PMMA/MAM + 1.5%SP, keeping the ratios of PMMA/MAM of the binary blends and adding a 1.5 wt% of sepiolites. In addition, a pure PMMA and a binary blend with sepiolites but without MAM were also produced for comparison.

The blends were produced with a twin-screw extruder COLLIN TEACH-LINE ZK 25T (L/D = 24, screw diameter = 25 mm). The materials were first dried in vacuum at 50 °C. The temperature profile in the extruder varied from 160 °C to 200 °C, and the screw speed was 40 rpm. The extruded material was cooled down in a water bath and pelletized. After drying, each formulation was extruded again to assure homogeneity. The filament from the second extrusion (thickness of 3–4 mm) was set aside and cut in cylindrical samples of 30 mm in length for the foaming experiments. MD direction in the filaments corresponds to the extrusion direction and TD direction is any direction perpendicular to it.

2.3. Gas dissolution foaming experiments

The foaming experiments were performed using a high-pressure vessel (PARR 4681, Parr Instrument Company). Pressure is controlled with a pressure pump controller (SFT-10, Supercritical Fluid Technologies Inc). A clamp heater of 1200 W and a CAL 3300 temperature controller allow the control of the temperature. A two-step foaming process was used [24]. The samples were put into the pressure vessel at a CO_2 pressure of 10 MPa and a temperature of 25 °C for the saturation stage during 20 h. Then, the pressure was abruptly released (pressure drop rate: 15 MPa/s). Finally, the samples were removed from the vessel and introduced into a thermal bath at 80 °C for 1 min for foaming. The time between the release of the pressure and the immersion of the samples in the bath was 2.5 min.

2.4. Characterization

The density of the solids (ρ_s) was measured with a gas pycnometer (AccuPyc II 1340, Micromeritics). The density of the cellular materials (ρ) was determined with the water-displacement method using a density determination kit for an AT261 Mettler-Toledo balance. More than 500 μm of the surface of cellular samples were removed with a polisher (LaboPOl2-LaboForce3, Struers) before measuring the densities. Relative density is defined as $\rho_r = \rho/\rho_s$.

The samples were fractured by cooling in liquid nitrogen for visualization and coated with gold using a sputter coater (SCD 005, Balzers Union). The surface morphology was analyzed using an ESEM Scanning Electron Microscope (QUANTA 200 FEG). The planes parallel (MD) and perpendicular (TD) to the extrusion direction were analyzed. The materials with sepiolites present a bimodal cellular structure with micro and nanometric cells, and the relative volume occupied by the population of nanometric cells, V_{nano}, was measured. The nanometric cells were fully characterized. The cell nucleation density (calculated using Kumar's approach [24]) was measured in the two planes ($N_{0,MD}$ and $N_{0,TD}$). The cell sizes were measured in two directions, calculating an average 3D cell size in the MD direction (ϕ_{MD}) and in the TD direction (ϕ_{TD}) with their corresponding standard deviations (*SD*) associated to the cell size distributions. For every single cell, the average anisotropy ratio in the MD direction was calculated as the ratio ϕ_{MD}/ϕ_{TD} [25,26], leading to an average anisotropy ratio value AR_{MD} and a standard deviation of the anisotropy ratio distribution (*SD*).

3. Results and discussion

3.1. Relative density

The relative density of the PMMA matrix in the foaming conditions used was 0.29 (Table 1), similar to that obtained when sepiolites are introduced in the system (0.26). The addition of MAM increases the relative density to values of 0.45 for 1% MAM content and to 0.56 for 10 wt% MAM. In the PMMA/MAM blends, nucleation takes place within the MAM micelles, that is, every micelle grows to become a cell. As a consequence of the molecular organization of the micelle, cells are restricted to grow spherically, and thus the expansion is these systems is limited [20,27]. The combination of MAM with sepiolites reduces the relative density for a MAM content of 1% (from 0.45 to 0.37) and maintains the relative density for the system containing a 10% of MAM.

3.2. Cellular structure

3.2.1. Binary blends: PMMA/MAM and PMMA/sepiolites

This section focusses on the behaviour of the binary blends. The addition of MAM to the PMMA matrix leads to a reduction of the cell size to the nanometric scale (Fig. 1.a–f and Table 1), and the higher the amount of MAM, the smaller the cell size [27]. Isotropic cellular structures in TD and MD planes are found for 1 wt% of MAM. However, the sample with 10 wt% of MAM shows an orientation of the cells in the extrusion direction, causing an anisotropic

Table 1
Characteristics of the materials produced in this work (*amount of MAM in the PMMA/MAM matrix). Cell sizes ϕ_{TD}, ϕ_{MD} and AR_{MD} show the averages, while values in brackets represent the *SD* of the cell size/anisotropy ratio distributions.

Series	MAM content* (wt%)	Sepiolite content (wt%)	ρ_r	V_{nano}(%)	$N_{0,TD}$ (nuclei/cm^3)	$N_{0,MD}$ (nuclei/cm^3)	ϕ_{TD}(nm)	ϕ_{MD}(nm)	AR_{MD}
PMMA/MAM	0	0	0.29 ± 0.02	100	$4.6{\cdot}10^{11}$	$5.6{\cdot}10^{11}$	1900 (±1500)	1700 (±1300)	0.96 (±0.45)
PMMA/MAM	1	0	0.45 ± 0.01	100	$5.2{\cdot}10^{14}$	$9.1{\cdot}10^{14}$	125 (±67)	128 (±72)	1.12 (±0.57)
PMMA/MAM	10	0	0.56 ± 0.01	100	$9.7{\cdot}10^{14}$	$6.3{\cdot}10^{14}$	96 (±59)	158 (±167)	1.71 (±1.25)
PMMA/MAM + 1.5%SP	0	1.5	0.26 ± 0.01	88	$1.4{\cdot}10^{14}$	$5.1{\cdot}10^{13}$	294 (±172)	509 (±379)	1.88 (±1.15)
PMMA/MAM + 1.5%SP	1	1.5	0.37 ± 0.00	96	$3.0{\cdot}10^{14}$	$1.6{\cdot}10^{14}$	189 (±127)	273 (±268)	1.48 (±0.86)
PMMA/MAM + 1.5%SP	10	1.5	0.57 ± 0.01	99	$1.2{\cdot}10^{15}$	$1.1{\cdot}10^{14}$	106 (±76)	288 (±365)	2.77 (±2.68)

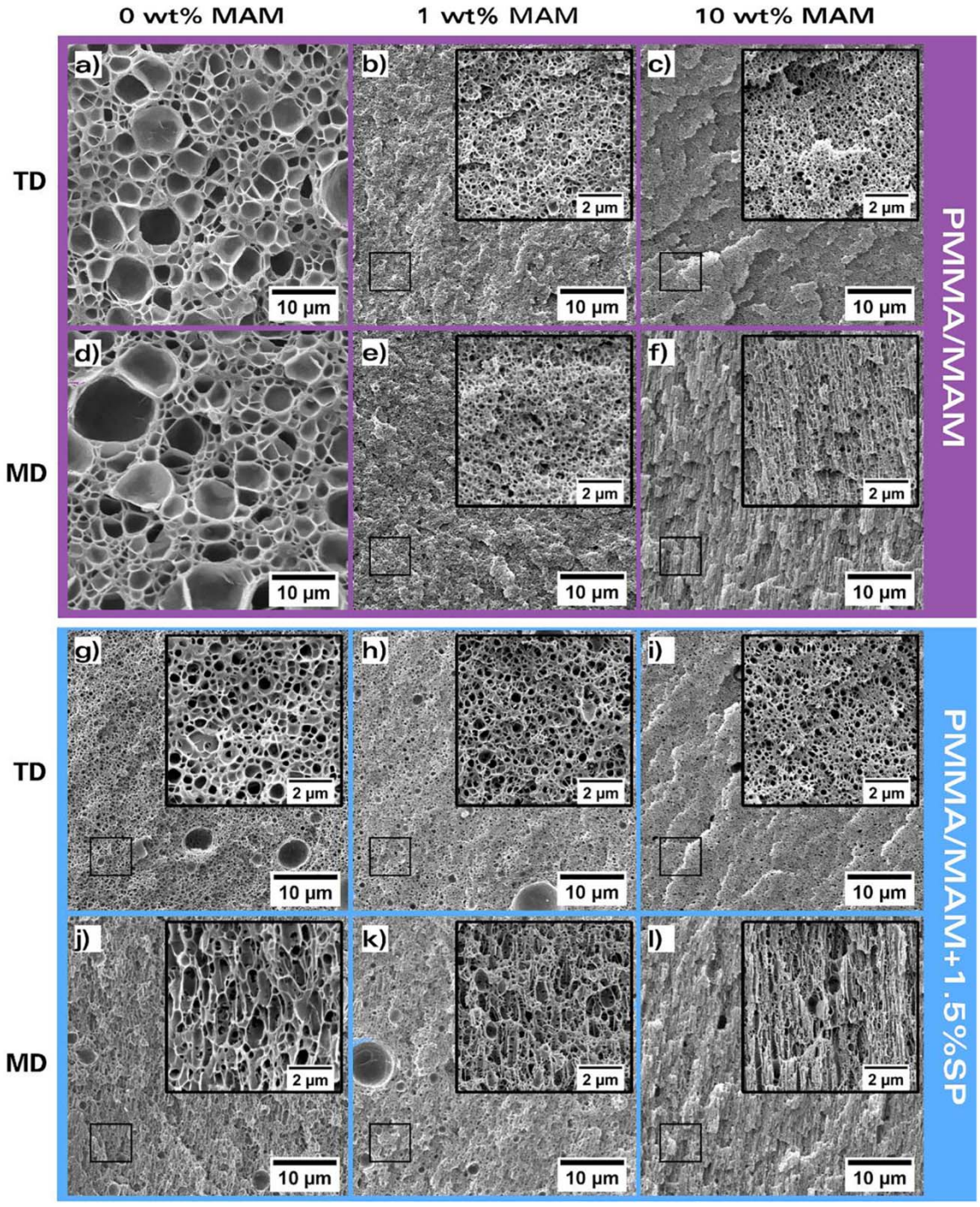

Fig. 1. SEM micrographs of: pure PMMA (a and d), PMAM/MAM blends (b, c, e and f), PMMA + 1.5%SP (g and j) and PMMA/MAM + 1.5%SP ternary blends (h, i, k and l). First and third rows: TD plane. Second and forth rows: MD plane.

structure (Fig. 1.f), whereas the TD surface is isotropic (Fig. 1.c). This effect was previously observed in PMMA/MAM by Pinto and coworkers [19], and it is a consequence of the alignment of the micelles due to the extrusion process. Nemoto et al. [28] also detected that aligned nanometric nucleants in the extruded solid resulted in aligned pores in the nanocellular material.

Regarding the materials with sepiolites, the addition of 1.5 wt% of particles (without MAM) produces a bimodal structure, due to the presence micron-sized aggregates and well-dispersed sepiolites, the structure being anisotropic in the MD plane (Fig. 1.g and j). In this case, the anisotropy is believed to be controlled by coalescence phenomena taking place along the sepiolites, which are aligned in the extrusion direction [22].

3.2.2. Tri-phasic blends with low content of MAM (1 wt%)

When the two nucleating agents are combined, intermediate effects are observed. For the system with 1 wt% of MAM, the addition of sepiolites implies a slight increase of the cell size, from around 130 nm to 190–270 nm and a reduction of the nucleation from 5 to $3{\cdot}10^{14}$ nuclei/cm^3 (in the TD plane) (Table 1). From the

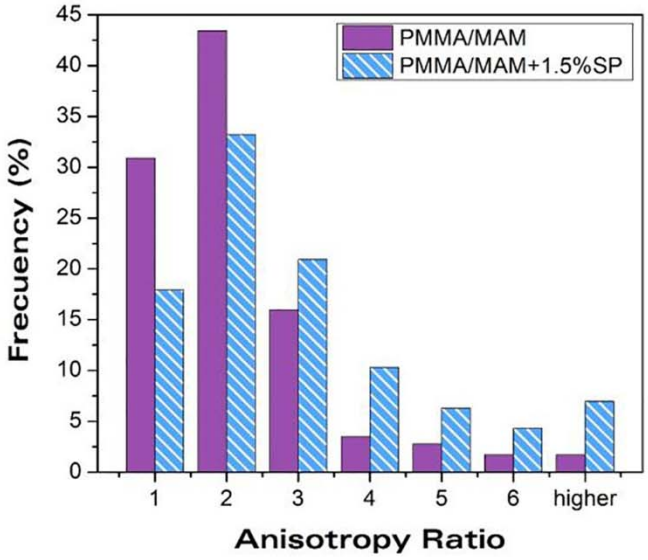

Fig. 2. Anisotropy ratio distribution in the MD direction for the materials with 10 wt% of MAM with and without sepiolites.

other perspective, the addition of 1 wt% of MAM to the sample with sepiolites increases the nucleation and reduces the cell size (from 290 to 510 to 190–270 nm) (Table 1). We conclude that with low contents of both nucleating agents there is a competition between the two, resulting in an intermediate nucleation density and cell size. Also, the relative density obtained in the tri-phasic system is in between those obtained in the binary blends as commented in section 3.1 because in this case the micelles are only partially limiting the expansion. However, the addition of sepiolites implies that anisotropic cells appear in the extrusion direction. The anisotropy ratio in the system with MAM and sepiolites is smaller than that in the system without MAM (1.48 versus 1.88) due to the presence of very small pores in the sample with MAM. In addition, the fraction of nanometric cells is slightly reduced by adding MAM (Table 1).

3.2.3. Tri-phasic blends with high content of MAM (10 wt%)

For 10 wt% of MAM, similar structures with and without sepiolites are observed in the TD plane (Fig. 1.c and i), with cell sizes around 100 nm and cell nucleation densities close to 10^{15} nuclei/cm^3 (Table 1). Then, when the fraction of MAM is 10 wt%, the effect of the sepiolites in the nucleation is no longer visible, and the micelle nanostructuration controls the nucleation. Regarding the presence of micrometric cells, the addition of a 10 wt% of MAM strongly avoids the formation of a bimodal structure (the fraction of nanometric cells increases, Table 1). However, sepiolites have an effect, and it is the increase in the anisotropy ratio in the MD direction (Fig. 1.l). As a consequence of the presence of the sepiolites, larger cells aligned in the extrusion direction appear, and anisotropy ratio increases from 1.7 to more than 2.7 when sepiolites are added (Table 1). In fact, not only the average anisotropy ratio is increased, but also the distribution of anisotropy ratios is wider, as seen in Fig. 2, meaning that in the system with MAM and sepiolites there are more cells with higher anisotropy ratios.

Fig. 3.a and b show schemes of the mechanisms of anisotropy formation in these systems. Without sepiolites (Fig. 3.a), anisotropy appears as a result of the alignment of the nanometric MAM micelles in the extrusion direction, inducing oriented coalescence. In the system with particles (Fig. 3.b) the presence of the needle-like sepiolites, which are long in comparison with the cell size, enhances the coalescence, leading to higher anisotropy ratios.

In a previous work, we proved that the addition of 10 wt% of sepiolites could induce the appearance of anisotropic cells with an average anisotropy ratio as high as 2.15 [22]. In this work, combining the action of aligned nanometric micelles in a PMMA/MAM matrix and oriented sepiolites particles it has been possible to

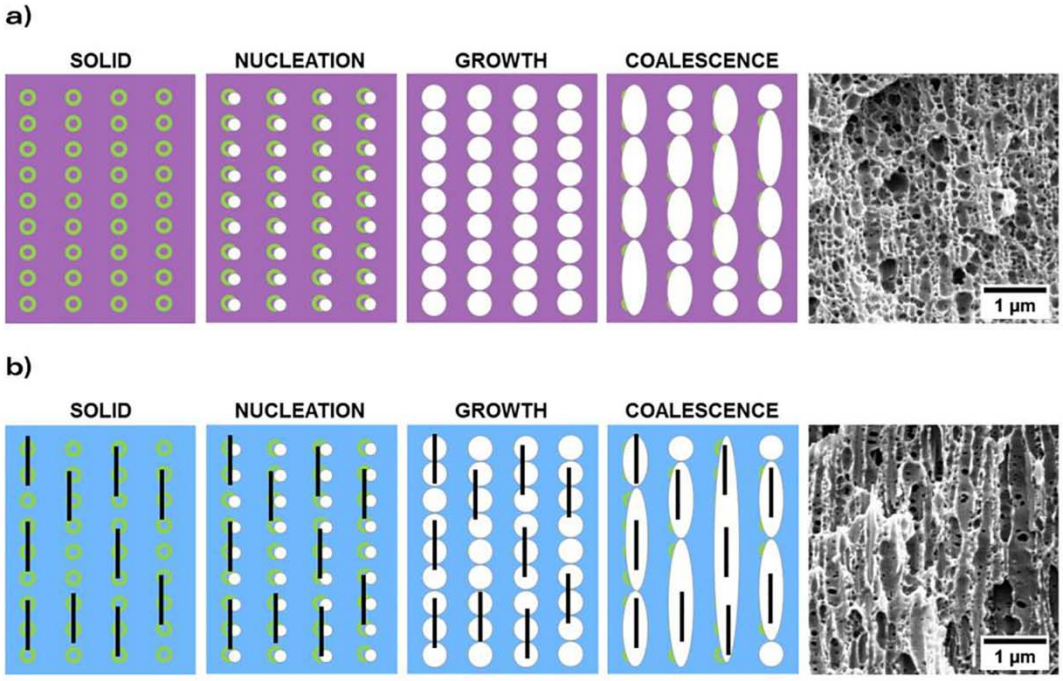

Fig. 3. a) Schematic representation of the formation of anisotropy in PMMA/MAM and b) PMMA/MAM + 1.5%SP. (Green circles: MAM micelles, black lines: sepiolites).

reach anisotropy ratios as high as 2.77 only using 1.5 wt% of sepiolites.

4. Conclusions

Highly anisotropic nanocellular materials based on PMMA/MAM with sepiolites have been produced by gas dissolution foaming. The nucleation mechanisms resulting from the addition of two different nucleating species have been also analyzed.

Results show that for low MAM contents (1 wt%), the nucleation in the PMMA/MAM + 1.5%SP system is in between those obtained in the samples with only one nucleating agent, meaning that none of the nucleants dominates, but the addition of sepiolites leads to the appearance of anisotropy in the MD direction (anisotropy ratio around 1.5). Regarding the system with high MAM content (10 wt %), nucleation is proved to be controlled by the MAM phase and not the sepiolites. The system without sepiolites presented already an anisotropic structure as a consequence of the aligned MAM micelles in the extrusion direction. However, the addition of sepiolites oriented in the same direction enhanced the anisotropy, leading to highly anisotropic structures with anisotropy ratios as high as 2.77.

Declaration of Competing Interest

The authors declare that they have no known competing financial interests or personal relationships that could have appeared to influence the work reported in this paper.

Acknowledgments

Financial support from the FPU grant FPU14/02050 (V. Bernardo) from the Spanish Ministry of Education and the Junta of Castile and Leon grant (J. Martín-de León) are gratefully acknowledged. Financial assistance from MINECO, FEDER, UE (MAT2015-69234-R), the Junta de Castile and Leon (VA275P18) and Spanish Ministry of Science, Innovation and Universities (RTI2018-098749-B-I00) are gratefully acknowledged. We would also like to thank Tolsa (Madrid, Spain) for supplying the sepiolites and Arkema for supplying the copolymers used in this research. Financial assistance from EREN (Ente Regional de la Energía de Castilla y León. EREN_2019_L4_UVA) is gratefully acknowledged.

References

[1] S. Costeux, CO2-blown nanocellular foams, J. Appl. Polym. Sci. 131 (2014) 41293(1)–41293(16), https://doi.org/10.1002/app.41293.
[2] S. Liu, J. Duvigneau, G.J. Vancso, Nanocellular polymer foams as promising high performance thermal insulation materials, Eur. Polym. J. 65 (2015) 33–45, https://doi.org/10.1016/j.eurpolymj.2015.01.039.
[3] B. Notario, J. Pinto, M.A. Rodriguez-Perez, Nanoporous polymeric materials: a new class of materials with enhanced properties, Prog. Polym. Sci. 78–79 (2016) 93–139, https://doi.org/10.1016/j.pmatsci.2016.02.002.
[4] G. Wang, C. Wang, J. Zhao, G. Wang, C.B. Park, G. Zhao, Modelling of thermal transport through a nanocellular polymer foam: Toward the generation of a new superinsulating material, Nanoscale 9 (2017) 5996–6009, https://doi.org/10.1039/c7nr00327g.
[5] Y. Fujimoto, S.S. Ray, M. Okamoto, A. Ogami, K. Yamada, K. Ueda, Well-controlled biodegradable nanocomposite foams: from microcellular to nanocellular, Macromol. Rapid Commun. 24 (2003) 457–461, https://doi.org/10.1002/marc.200390068.
[6] S. Liu, B. Zoetebier, L. Hulsman, Y. Zhang, J. Duvigneau, G.J. Vancso, Nanocellular polymer foams nucleated by core-shell nanoparticles, Polymer (Guildf). 104 (2016) 22–30, https://doi.org/10.1016/j.polymer.2016.09.016.
[7] H. Yu, Y. Lei, X. Yu, X. Wang, T. Liu, S. Luo, Solid-state polyetherimide (PEI) nanofoams: the influence of the compatibility of nucleation agent on the cellular morphology, J. Polym. Res. 23 (2016) 121, https://doi.org/10.1007/s10965-016-1009-2.
[8] L. Urbanczyk, C. Calberg, C. Detrembleur, C. Jérôme, M. Alexandre, Batch foaming of SAN/clay nanocomposites with scCO2: a very tunable way of controlling the cellular morphology, Polymer (Guildf) 51 (2010) 3520–3531, https://doi.org/10.1016/j.polymer.2010.05.037.
[9] A. Ameli, M. Nofar, C.B. Park, Polypropylene/carbon nanotube nano/microcellular structures with high dielectric permittivity, low dielectric loss, and low percolation threshold, Carbon N. Y. 71 (2014) 206–207, https://doi.org/10.1016/j.carbon.2014.01.031.
[10] J. Pinto, D. Morselli, V. Bernardo, B. Notario, D. Fragouli, M.A. Rodriguez-Perez, A. Athanassiou, Nanoporous PMMA foams with templated pore size obtained by localized in situ synthesis of nanoparticles and CO2 foaming, Polymer (Guildf) 124 (2017) 176–185, https://doi.org/10.1016/j.polymer.2017.07.067.
[11] T. Nemoto, J. Takagi, M. Ohshima, Nanoscale cellular foams from a poly (propylene)-rubber blend, Macromol. Mater. Eng. 293 (2008) 991–998, https://doi.org/10.1002/mame.200800184.
[12] C. Forest, P. Chaumont, P. Cassagnau, B. Swoboda, P. Sonntag, CO2 nanofoaming of nanostructured PMMA, Polymer (Guildf) 58 (2015) 76–87, https://doi.org/10.1016/j.polymer.2014.12.048.
[13] G. Wang, J. Zhao, L.H. Mark, G. Wang, K. Yu, C. Wang, C.B. Park, G. Zhao, Ultra-tough and super thermal-insulation nanocellular PMMA/TPU, Chem. Eng. J. 325 (2017) 632–646, https://doi.org/10.1016/j.cej.2017.05.116.
[14] R.W.B. Sharudin, M. Ohshima, CO2-induced mechanical reinforcement of polyolefin-based nanocellular foams, Macromol. Mater. Eng. 296 (2011) 1046–1054, https://doi.org/10.1002/mame.201100085.
[15] T. Otsuka, K. Taki, M. Ohshima, Nanocellular foams of PS/PMMA polymer blends, Macromol. Mater. Eng. 293 (2008) 78–82, https://doi.org/10.1002/mame.200700257.
[16] C. Dutriez, K. Satoh, M. Kamigaito, H. Yokoyama, Nanocellular foaming of fluorine containing block copolymers in carbon dioxide: the role of glass transition in carbon dioxide, RSC Adv. 2 (2012) 2821–2827, https://doi.org/10.1039/c2ra01268e.
[17] S. Costeux, L. Zhu, Low density thermoplastic nanofoams nucleated by nanoparticles, Polymer (Guildf). 54 (2013) 2785–2795, https://doi.org/10.1016/j.polymer.2013.03.052.
[18] J.A. Reglero Ruiz, M. Dumon, J. Pinto, M.A. Rodriguez-Perez, Low-density nanocellular foams produced by high-pressure carbon dioxide, Macromol. Mater. Eng. 296 (2011) 752–759, https://doi.org/10.1002/mame.201000346.
[19] J. Pinto, M. Dumon, M. Pedros, J. Reglero, M.A. Rodriguez-Perez, Nanocellular CO2 foaming of PMMA assisted by block copolymer nanostructuration, Chem. Eng. J. 243 (2014) 428–435, https://doi.org/10.1016/j.cej.2014.01.021.
[20] V. Bernardo, J. Martin-de Leon, E. Laguna-Gutierrez, T. Catelani, J. Pinto, A. Athanassiou, M.A. Rodriguez-Perez, Understanding the role of MAM molecular weight on the production of PMMA/MAM nanocellular polymers, Polymer (Guildf) 153 (2018) 262–270, https://doi.org/10.1016/j.polymer.2018.08.022.
[21] V. Bernardo, J. Martin-de León, E. Laguna-Gutiérrez, M.Á. Rodríguez-Pérez, PMMA-sepiolite nanocomposites as new promising materials for the production of nanocellular polymers, Eur. Polym. J. 96 (2017) 10–26, https://doi.org/10.1016/j.eurpolymj.2017.09.002.
[22] V. Bernardo, J. Martin-de Leon, M.A. Rodriguez-Perez, Anisotropy in nanocellular polymers promoted by the addition of needle-like sepiolites, Polym. Int. 68 (2019) 1204–1214, https://doi.org/10.1002/pi.5813.
[23] J. Santaren, A. Alvarez, A. Esteban-Cubillo, B. Notario, D. Velasco, M.A. Rodrıguez-Perez, Improving the cellular structure and thermal conductivity of PS foams by using Sepiolites, in: Foams 2012, 2012, pp. 1–5.
[24] V. Kumar, N.P. Suh, A process for making microcellular parts, Polym. Eng. Sci. 30 (1990) 1323–1329, https://doi.org/10.1002/pen.760302010.
[25] A.T. Huber, L.J. Gibson, Anisotropy of foams, J. Mater. Sci. 23 (1988) 3031–3040, https://doi.org/10.1007/BF00547486.
[26] J. Xu, T. Wu, J. Zhang, H. Chen, W. Sun, C. Peng, Microstructure measurement and microgeometric packing characterization of rigid polyurethane foam defects, Cell. Polym. 36 (2017) 183–204, https://doi.org/10.1177/026248931703600402.
[27] V. Bernardo, J. Martin-de Leon, J. Pinto, T. Catelani, A. Athanassiou, M.A. Rodriguez-Perez, Low-density PMMA/MAM nanocellular polymers using low MAM contents: Production and characterization, Polymer (Guildf) 163 (2019) 115–124, https://doi.org/10.1016/j.polymer.2018.12.057.
[28] T. Nemoto, J. Takagi, M. Ohshima, Nanocellular foams—cell structure difference between immiscible and miscible PEEK/PEI polymer blends, Polym. Eng. Sci. 50 (2010) 2408–2416, https://doi.org/10.1002/pen.